Golgi retention of KIT in gastrointestinal stromal tumour cells is phospholipase D activity-dependent

Yuuki Obata[1], Miyuki Natsume[1,2], Isamu Shiina[2], Tsuyoshi Takahashi[3], Toshirou Nishida[4]

[1]Laboratory of Intracellular Traffic & Oncology, National Cancer Center Research Institute, Tsukiji, Chuo-ku, Tokyo 104-0045, Japan; [2]Department of Applied Chemistry, Faculty of Science, Tokyo University of Science, Shinjuku-ku, Tokyo 162-8601, Japan; [3]Department of Gastroenterological Surgery, Graduate School of Medicine, Osaka University, Suita, Osaka 565-0871, Japan; [4]National Cancer Center Hospital, Tsukiji, Chuo-ku, Tokyo 104-0045, Japan

[*]**Corresponding author**: Yuuki Obata, Ph.D.
Laboratory of Intracellular Traffic & Oncology
National Cancer Center Research Institute
Tsukiji, 5-1-1, Chuo-ku
Tokyo 104-0045, Japan
Tel: +81-3-3547-5201 / Fax: +81-3-3542-2530
Email: yuobata@ncc.go.jp

Grant Support

Japan Society for the Promotion of Science (24K10370 to Y. O. and 22K08883 to T. N.)

The Research Foundation for Pharmaceutical Sciences (to Y. O.)

Japan Foundation for Applied Enzymology (to Y. O.)

Life Science Foundation of JAPAN (to Y. O.)

Foundation for Promotion of Cancer Research (to Y. O.)

Email

Miyuki Natsume	g.s.miyunatsu@gmail.com
Isamu Shiina	shiina@rs.tus.ac.jp
Tsuyoshi Takahashi	takahashi.tsuyoshi.med@osaka-u.ac.jp
Toshirou Nishida	tnishida@ncc.go.jp

Abstract

A constitutively active mutant of the receptor protein-tyrosine kinase KIT is a major cause of gastrointestinal stromal tumours (GISTs). Recently, we discovered that during biosynthetic transport, the KIT mutant (KIT^{mut}) is retained in the Golgi/*trans*-Golgi network (TGN), where it activates downstream molecules. This retention is dependent on the phospholipase Cγ2–protein kinase D2–PI4 kinase IIIβ (PLCγ2–PKD2–PI4KIIIβ) pathway, which KIT^{mut} activates at the Golgi/TGN. The activated cascade aberrantly recruits GGA1 and the γ-adaptin subunit of AP1, resulting in KIT^{mut} retention in the Golgi/TGN. However, the precise mechanisms, including the mediators and effectors in the pathway, remain unclear. In humans, the phosphatidic acid-generating enzymes, phospholipase D1 (PLD1) and PLD2, are known downstream proteins of PKD. In the presence of the PLD inhibitor CAY10594, KIT^{mut} is released from the Golgi/TGN and subsequently degraded in lysosomes, leading to signal inactivation. Knockdown experiments indicated that PLD2 plays a role in KIT^{mut} retention. KIT^{mut} activates PLD2 through PKD2, but not PI4KIIIβ, for Golgi/TGN retention. PLD activity is required for the association of γ-adaptin with GGA1. Therefore, the KIT–PLCγ2–PKD2 pathway separately activates PLD2 and PI4KIIIβ to recruit γ-adaptin and GGA1. Collectively, these results suggest that KIT^{mut} retention is dependent on the activation of the PLCγ2–PKD2–PLD2 cascade in GIST.

Keywords: RTK, KIT, GIST, Golgi/TGN, PKD, PLD

47 **Introduction**

48 The stem cell factor (SCF) receptor, KIT, is a type III receptor protein-tyrosine kinase (RTK) that
49 is primarily located in the plasma membrane (PM) of the interstitial cells of Cajal in the
50 gastrointestinal tract, as well as in haematopoietic cells, mast cells, melanocytes, and germ cells
51 in the testis[1–3]. Upon SCF binding to the PM, KIT dimerises, resulting in enhanced protein
52 tyrosine kinase activity. This, in turn, activates several signalling molecules, such as AKT,
53 extracellular signal-regulated kinase, phospholipase Cγ (PLCγ), and signal transducer and
54 activator of transcription (STAT) proteins, leading to cell growth, survival, migration, and
55 differentiation[1]. Consequently, the constitutive activation of KIT through genetic abnormalities,
56 such as point mutations and in-frame deletions, plays a critical role in cancerogenesis. Indeed,
57 most cases of mast cell leukaemia in adult humans, as well as patients with gastrointestinal
58 stromal tumours (GISTs), harbour KIT mutations[4–7]. As a result, imatinib, a KIT inhibitor
59 (tyrosine kinase inhibitor (TKI)), has been used to treat patients with advanced GISTs. However,
60 2–3 years after the administration of imatinib, TKIs become ineffective in the treatment of
61 advanced GISTs[8–10]. In most cases, mutations conferring imatinib resistance are found in the *KIT*
62 gene.

63 Previously, we reported that, unlike normal KIT, mutant KIT (KIT^{mut}) in leukaemia cells and
64 GIST is localised to intracellular compartments where it can be autophosphorylated and
65 activated[11–15]. Moreover, the localisation of the mutant in leukaemia cells is notably different from
66 that in GIST cells; in leukaemia cells, KIT^{mut} accumulates in the endosome–lysosome
67 compartments[11, 13, 15], whereas in GIST cells, it is retained in the Golgi/*trans*-Golgi network

68 (Golgi/TGN) area during biosynthesis[12, 14]. In both cases, KIT^{mut} localises to intracellular
69 compartments depending on its tyrosine kinase activity[11, 12, 15]. We recently demonstrated that
70 KIT^{mut} retention depends on protein kinase D2 (PKD2) activity in GIST cells[16]. The mediator
71 between KIT^{mut} and PKD2 is PLCγ2. It was suggested that the KIT–PLCγ2–PKD2 pathway
72 activates the phosphatidylinositol 4-phosphate-producing (PI4P-producing) enzyme PI4 kinase
73 IIIβ (PI4KIIIβ), leading to the aberrant recruitment of Golgi-localised, γ-ear-containing, ARF-
74 binding family of protein 1 (GGA1) and an adaptor protein-1 complex (AP1) component γ-
75 adaptin. Subsequently, KIT itself is retained in the Golgi/TGN area. These findings raised several
76 questions: How do the aberrantly recruited AP1 and GGA1 trap KIT in the Golgi/TGN?; Are
77 there PKD2 effectors other than PI4KIIIβ? These questions remain unresolved.

78 Several studies have suggested that PKD enhances phosphatidylcholine-selective
79 phospholipase D (PC-PLD; hereafter referred to as PLD) activity to generate phosphatidic acid
80 (PA) from PC on the cytoplasmic face of the PM and Golgi/TGN membrane[17–19]. Under normal
81 conditions, PA plays a key role in forming transport carriers in the Golgi/TGN membrane[20–25]. It
82 creates a negative curvature at the budding site of membrane carriers due to its cone-like shape
83 and provides a hydrophobic zone as a scaffold region for functional proteins[26–28]. Human PLDs
84 consist of six structurally related proteins: PLD1, PLD2, PLD3, PLD4, PLD5, and PLD6. PLD1
85 and PLD2 are crucial for membrane carrier formation through PLD activity, while PLD3, PLD4,
86 and PLD5 lack canonical phospholipase activity and may possess endonuclease activity in
87 lysosomes and the endoplasmic reticulum (ER)[28, 29]. PLD6 is localised in mitochondria to produce
88 PA from cardiolipins. Therefore, we hypothesised that the KIT–PLCγ2–PKD2 pathway activates
89 PLD1 and/or PLD2, and that aberrant PA production leads to the mutant receptor's retention in

90 the Golgi/TGN in GIST cells.

91 The present study aimed to determine the requirement of PLD activity for Golgi/TGN
92 retention of KIT^{mut} in GIST cells by investigating the relationship between the PLCγ2–PKD2
93 pathway and PLDs using PLD inhibitors, knockdown experiments, immunofluorescence confocal
94 microscopic analysis, and biochemical assays.

Results

KIT^{mut} is retained in the Golgi/TGN region depending on PLD activity in GIST cells

Previous studies have shown that PLD and PI4KIIIβ are activated downstream of PKD[17–19]. We hypothesised that PLD activity was also involved in the retention of KIT^{mut} in the Golgi/TGN region of GIST cells. To evaluate this hypothesis, we treated GIST-T1 cells, which endogenously express a constitutively active KIT$^{\Delta 560–578}$ mutant (imatinib-sensitive)[30], with CAY10594 (an inhibitor of PLD activity)[31, 32] and examined whether PLD inhibition mimicked the inhibition of PKD2 on KIT localisation and growth signalling. First, we performed an immunofluorescence confocal microscopic assay with anti-KIT and anti-golgin97 (TGN marker) antibodies in GIST-T1 cells treated with 20 μM CAY10594. As shown in Figure 1a, KIT was found in the Golgi/TGN area together with golgin97 under normal conditions (upper panels), whereas it was absent in CAY10594-treated cells (lower panels). This effect of CAY10594 was similar to that of the PKD inhibitor CRT0066101 in releasing KIT from the Golgi/TGN region (compare Fig. 1a with Suppl. Fig. 1a). Immunoblotting revealed that CAY10594 treatment decreased KIT protein levels in a time- and dose-dependent manner (Fig. 1b, upper panels). This effect was similar to that of PKD2 inhibition by CRT0066101 and small interfering RNA (siRNA), which induce the degradation of KIT in lysosomes[16]. Under PLD-inhibited conditions, the KIT downstream proteins, AKT and STAT5, were dephosphorylated and inactivated (Fig. 1b). Treatment with other PLD inhibitors, such as 1-butanol[20, 33, 34], gave similar results (Fig. 1c). These results suggest that PLD activity is required for KIT^{mut} signalling by trapping the mutant in the Golgi/TGN region. Importantly, neither CAY10594 nor 1-butanol decreased phospho-PKD2 S876 (pPKD2^{S876}) levels (Fig. 1b, c),

116 indicating that PKD2 is not a downstream molecule of PLD2. Next, we examined the effect of
117 PLD inhibition with CAY10594 in imatinib-resistant GIST cell lines, GIST-R9 (*KIT*$^{\Delta 560–578,D820V}$)
118 and GIST430 cells (*KIT*$^{\Delta 560–576,V654A}$). Although higher concentrations of the compound were
119 required, GIST-R9 and GIST430 cells showed results similar to those of CAY10594-treated
120 GIST-T1 cells; the protein levels of KIT decreased, AKT and STAT5 were dephosphorylated, and
121 pPKD2^{S876} was not reduced (Fig. 1d; Suppl. Fig. 1b). Taken together, these results suggest that
122 PLD, a presumed PKD effector, plays a key role in Golgi/TGN retention of KIT^{mut}.

123 **KIT^{mut} released from the Golgi/TGN migrates to lysosomes in GIST cells**

124 Recently, we reported that in PKD2-inhibited GIST cells, KIT^{mut} is released from the Golgi/TGN
125 region into the PM and is subsequently degraded in lysosomes[16]. To examine whether CAY10594-
126 induced KIT reduction was lysosome-dependent, we treated GIST-T1 cells with CAY10594 and
127 ammonium chloride (NH_4Cl), which inhibits lysosomal proteases[35], followed by immunoblotting.
128 Figure 2a shows that CAY10594 alone decreased the protein level of KIT, whereas the level of
129 KIT was restored in cells treated with CAY10594 and NH_4Cl. The levels of transferrin receptor,
130 which circulates between the PM and endosomes[36], were not affected by these treatments,
131 suggesting that CAY10594 specifically acts on KIT^{mut} trafficking. In support of these results,
132 immunofluorescence data showed that in the presence of CAY10594 and NH_4Cl, KIT was found
133 in the lysosome-associated membrane protein 1-positive area (Fig. 2b). CAY10594, therefore, has
134 an effect similar to that of PKD2 inhibition on the distribution of KIT^{mut} in GIST cells. These
135 results suggest that KIT^{mut} is degraded in lysosomes after CAY10594-induced release from the
136 Golgi/TGN region.

137 **PLD2 knockdown phenocopies the effect of CAY10594 treatment in GIST-T1 cells**

138 Mammalian PLDs comprise six structurally related proteins: PLD1, PLD2, PLD3, PLD4, PLD5,
139 and PLD6[29,37]. PLD1 and PLD2 have PA-producing PLD activity not only in the PM but also in
140 the Golgi/TGN, whereas no canonical PLD activity of PLD3, PLD4, or PLD5 has been reported[29].
141 PLD6 hydrolyses cardiolipin to generate PA in the mitochondria and is called mito-PLD.
142 Therefore, we examined whether the knockdown of PLD1 or PLD2 phenocopied the effect of
143 chemical inhibition of PLD in GIST. In PLD2-knockdown GIST-T1 cells, KIT reduction, a sign
144 of release from the Golgi/TGN region, and suppression of KIT signalling were observed (Fig. 3a).
145 Similar to the CAY10594 treatment, PLD2 knockdown did not decrease the expression of
146 $pPKD2^{S876}$. PLD1 protein expression was not detected in this cell line; thus, PLD1 siRNA had no
147 effect on KIT retention or growth signalling. Therefore, PLD2 plays a pivotal role in Golgi/TGN
148 retention of KIT in GIST-T1 cells. At this stage, we could not determine whether PLD1 was
149 important for KIT retention. Next, we investigated whether PLD2 is downstream of KIT^{mut}. As
150 shown in Figure 3b, imatinib, a KIT tyrosine kinase inhibitor, markedly decreased the
151 phosphorylation of PLD2 both at residues Y169 and Y511, which are signs of PLD2 activation.
152 Furthermore, PLD2 coimmunoprecipitated with KIT and vice versa, and this interaction was
153 suppressed by imatinib treatment (Fig. 3c). These results suggest that PLD2 is located
154 downstream of KIT^{mut} in GIST-T1 cells.

155 Next, we examined the subcellular localisation of PLD2. In our immunofluorescence assay,
156 we were unable to detect endogenous PLD2, probably due to the low ability of the antibodies.
157 Transiently transfected MYC-tagged PLD2 was found not only in the Golgi/TGN region but also
158 in other endomembranes (Suppl. Fig. 2), indicating that a small fraction of PLD2 is associated

159 with KIT^{mut} in GIST cells.

160 We next examined whether PLD knockdown had a similar effect on RTK^{mut} expression in
161 leukaemia cells as on KIT^{mut} expression in GIST-T1 cells. We previously reported that KIT^{mut} in
162 AML cells (Kasumi-1) and MCL cells (HMC-1.2) flows normally from the Golgi/TGN to the PM
163 and immediately moves to the endosome–lysosome compartments[11, 13, 15]. We were unable to
164 determine the expression of PLD2 and PLD1 in Kasumi-1 and HMC-1.2 cells, respectively. As
165 shown in Figure 3d, compared with KIT in GIST-T1 cells, KIT in Kasumi-1 and HMC-1.2 was
166 not decreased by PLD knockdown. In addition, we recently showed that in AML cells, the FLT3
167 internal tandem duplication (FLT3-ITD) mutant is retained in the Golgi/TGN, where it initiates
168 the activation of AKT[38]. It activates STAT5 in the ER[38, 39], suggesting that FLT3-ITD signalling
169 occurs during its biosynthetic trafficking. The knockdown of PLD1 or PLD2 did not affect the
170 protein levels of FLT3 or AKT activation in the AML cell line MOLM-14 (Fig. 3e). Furthermore,
171 FLT3-ITD-dependent STAT5 activation in the ER was unaffected in PLD-knockdown cells. This
172 supports our findings that Golgi/TGN retention in FLT3-ITD is a PKD2-independent manner[16].
173 Collectively, these results suggest that PLD activity is specifically involved in Golgi/TGN
174 retention of KIT^{mut} in GIST cells.

175 **KIT–PLCγ2–PKD2 separately activates PI4KIIIβ and PLD2**

176 Finally, we asked where PLD2 is located in the KIT–PLCγ2–PKD2–PI4KIIIβ–AP1–GGA1
177 pathway. Figure 4a shows that the knockdown of PLCγ2 as well as PKD2 reduced the $pPLD2^{Y511}$,
178 supporting previous reports that PLDs are downstream molecules of PKD[17–19]. On the other hand,
179 $pPLD2^{Y511}$ was maintained in PI4KIIIβ-knocked down cells compared with PKD2-knocked down

180 cells, indicating that PLD2 is not a downstream molecule of PI4KIIIβ. Next, we examined PI4P
181 levels in the Golgi/TGN region. Imatinib (KIT inhibitor), CRT0066101 (PKD inhibitor), and PIK-
182 93 (PI4KIIIβ inhibitor) decreased PI4P in the Golgi/TGN region (Fig. 4b), consistent with our
183 previous report. On the other hand, PI4P was found in the Golgi/TGN area in CAY10594 (PLD
184 inhibitor). Our recent study showed that activation of the KIT–PLCγ2–PI4KIIIβ pathway is a
185 cause of the association of γ-adaptin and GGA1. As shown in Figure 4c, inhibition of PI4KIIIβ,
186 PKD2, and PLD2 decreased γ-adaptin interaction with GGA1. Collectively, these results suggest
187 that PKD2 separately activates PLD2 and PI4KIIIβ to recruit AP1 and GGA1. Both PI4KIIIβ-
188 produced PI4P and PLD2-produced PA probably contribute to the association of AP1 with GGA1.
189 We found that the imatinib-resistant GIST cell lines, GIST-R9 and GIST430, expressed PLD1,
190 unlike GIST-T1 cells. PLD2 knockdown partially decreased the protein levels of KIT in these
191 cells compared with PLD2-knocked down GIST-T1 cells (Suppl. Fig. 3a). In GIST430 cells, the
192 knockdown of PLD1 decreased KIT by 10%, indicating that the involvement of PLD1 in KIT
193 retention depends on the cell context. AKT and STAT5 phosphorylation was not reduced in PLD1-
194 or PLD2-knocked down cells. Although pSTAT5 was partially decreased, simultaneous
195 knockdown of PLD1 and PLD2 in GIST-R9 and GIST430 cells did not affect KIT levels or pAKT
196 to a similar extent as in GIST-T1 cells (Suppl. Fig. 3b). These imatinib-resistant GIST cells may
197 compensate for the loss of PLD1 and PLD2 proteins and restore PA levels in PLD1/PLD2-
198 knocked down cells. At present, we cannot explain the reason for this. Further studies are required
199 to elucidate these compensation mechanisms.

200 **Discussion**

201 In this study, we demonstrated that PLD activity was required for Golgi/TGN retention by KIT^{mut}
202 in GIST (Fig. 4d). The PLD inhibitors CAY10594 and 1-butanol move KIT^{mut} from the
203 Golgi/TGN, resulting in downstream inactivation. After release from the Golgi/TGN region,
204 KIT^{mut} is incorporated into lysosomes for degradation. PLD inhibitors have a similar effect as
205 PKD inhibitors on KIT^{mut} localisation and growth signalling in GIST cells. KIT^{mut} activates PLD2
206 via the PLCγ2–PKD2 pathway. PKD2 could separately activate PLD2 and PI4KIIIβ for
207 producing PA and PI4P, respectively. Both PLD2 and PI4KIIIβ are required for the association
208 of AP1 with GGA1, which is a cause of Golgi retention of KIT^{mut} in GIST cells. The loss-of-
209 function of PLD does not affect the signalling of other RTK^{mut} mutations such as FLT3-ITD in
210 AML. These findings suggest that KIT^{mut} separately activates PLD2 and PI4KIIIβ through the
211 PLCγ2–PKD2 pathway for its Golgi retention in GIST cells.

212 Previous studies have demonstrated Golgi/TGN retention by RTKs other than KIT^{mut} and
213 FLT3-ITD. Constitutively active forms of PDGFRA, FGFR3, and TRKA are found in the
214 Golgi/TGN region and are autophosphorylated in cancer cells[40–44]. In hepatocellular carcinoma
215 cells, overexpressed MET was retained in the Golgi/TGN region in a manner dependent on its
216 tyrosine kinase activity[45]. Tyrosine phosphorylates the HER3 kinase, leading to the autonomous
217 proliferation of host cells. Non-receptor-type oncogenic proteins, such as Src-family tyrosine
218 kinases, RAS GTPases, and mammalian target of rapamycin, have been suggested to use the
219 Golgi/TGN membrane as their signalling platform[46–51]. In particular, PLD is located downstream
220 of RAS[52, 53]. Investigating whether RAS uses PLD for Golgi/TGN localisation is attractive.

221 Therefore, it is of substantial interest to determine whether PLD plays a role in Golgi/TGN
222 retention of oncogenic signal transduction proteins other than GIST KIT^{mut}.

223 PLD1 and PLD2 generate PA and choline from PC located in the lipid bilayer[37]. PA plays
224 multiple roles in various cellular events, including lipid biogenesis, membrane trafficking,
225 cytoskeletal reorganisation, and acts as a scaffold for signal transduction[54–56]. In the transport
226 carrier formation process at the Golgi/TGN membrane, PA provides platforms for membrane
227 trafficking proteins and creates membrane curvature owing to its cone-like shape[26–28]. In GIST
228 cells, autophosphorylation of KIT in the Golgi/TGN membrane, which does not occur in normal
229 cells, aberrantly activates PLD2 via the PLCγ2–PKD2 pathway, probably resulting in local
230 dysregulated PA production. We hypothesised that abnormal local PA production would stop the
231 export of KIT^{mut} from the Golgi/TGN region. Abnormally generated PA may play a role in the
232 induction of the AP1–GGA1 interaction, which is involved in KIT retention. Analysis of PA
233 distribution with fluorescence imaging and quantification of PA amounts will help us understand
234 the precise mechanism of PA-dependent Golgi/TGN retention by KIT^{mut} in GIST cells.

235 In the present study, we identified PLD2 as a protein downstream of KIT^{mut} in GIST.
236 Previously, several groups reported that in mast cells, SCF-stimulated normal KIT at the PM
237 induces PLD activation, resulting in chemical mediator release[57, 58]. These studies suggest that the
238 SCF–KIT axis physiologically activates PLD in haematopoietic cells, melanocytes, germ cells in
239 the testes, and interstitial Cajal cells. Therefore, there is great interest in examining the
240 physiological role of PLD in these cells.

241 Previous studies reported that ADP-ribosylation factor (ARF) proteins act as mediators
242 between PKD and PLD[17–19, 59, 60]. In our recent report, we knocked down Golgi-localised ARFs

243 such as ARF1, ARF4, and ARF5 in GIST-T1 cells[61]. However, knockdown of ARF1, ARF4, or
244 ARF5 did not phenocopy PLD2 knockdown. Furthermore, since the simultaneous knockdown of
245 ARF1, ARF4, and ARF5 blocks the ER export of KIT^{mut}, a conclusion cannot be drawn from a
246 simple ARF loss-of-function study. Cell-free system methods and protein–protein interaction
247 analyses will be powerful tools for understanding the precise mechanism of PLD activation
248 through ARF function.

249 In imatinib-resistant GIST cell lines, knockdown of PLD1 and PLD2 could not fully explain
250 the effect of the PLD inhibitor CAY10594. Genetic alterations occur not only in the *KIT* gene[62].
251 Multiple enzymes such as diacylglycerol kinases, lysophosphatidic acid acyltransferase, PA
252 phosphatases, and phospholipase A are involved in controlling intracellular PA levels[28, 63]. In
253 GIST-R9 and GIST430 cells, alterations in the expression of PA-related proteins may compensate
254 for the loss of PLD1 and PLD2 by siRNA. Further studies are required to understand the
255 mechanisms underlying Golgi retention by KIT^{mut} in imatinib-resistant cells.

256 In conclusion, we showed that in addition to PI4KIIIβ, PLD2 is an effector protein of the
257 KIT–PLCγ2–PKD2 cascade, and its enzymatic product PA may be a key player for KIT retention
258 in the Golgi/TGN in GIST cells. PLD2 maintains the uncontrolled growth signalling of KIT^{mut} by
259 trapping the mutant in the Golgi/TGN. Our findings provide new insights into the role of PLD2
260 in GIST growth. Moreover, from a clinical perspective, our findings offer a new strategy for GIST
261 treatment by releasing KIT^{mut} from the signalling platform.

262 **Materials and Methods**

263 **Cell culture**

264 GIST-T1 cells (Cosmo Bio, Tokyo, Japan) and GIST-R9 cells were cultured at 37°C in Dulbecco's
265 modified Eagle's medium (DMEM) supplemented with 10% fetal calf serum (FCS), penicillin,
266 and streptomycin (Pen/Strep). GIST-R9 cells were incubated with 1 μM imatinib as described
267 previously[62]. GIST430/654 (hereafter referred to as GIST430) cells were kindly provided by Dr.
268 Jonathan Fletcher (Dana-Farber Cancer Institute, Boston, MA, USA). GIST430 cells were
269 cultured at 37°C in Iscove's modified Dulbecco's medium (IMDM) supplemented with 15% FCS
270 and Pen/Strep. GIST430 cells were maintained in the presence of 100 nM imatinib[64]. Kasumi-1
271 (JCRB Cell Bank, Osaka, Japan), MOLM-14 (DSMZ, Braunschweig, Germany), and HMC-1.2
272 cells[65] were cultured at 37°C in RPMI1640 supplemented with 10% FCS and Pen/Strep. All
273 human cell lines were authenticated by short tandem repeat analysis at the JCRB Cell Bank and
274 tested for *mycoplasma* contamination using a MycoAlert Mycoplasma Detection Kit (Lonza,
275 Basel, Switzerland).

276 **Antibodies**

277 The antibodies used for immunoblotting, immunoprecipitation, and immunofluorescence are
278 listed in Supplementary Table 1.

279 **Chemicals**

280 CAY10594, imatinib mesylate (Cayman Chemical, Ann Arbor, MI, USA), PIK-93, and
281 CRT0066101 (Selleck Chemicals) were dissolved in dimethyl sulfoxide. NH_4Cl and 1-butanol

282 were purchased from Sigma-Aldrich (St. Louis, MO) and Fujifilm Wako Chemicals (Osaka,
283 Japan), respectively.

284 **Gene silencing with siRNA**

285 For silencing, *PLD1*, *PLD2*, *PLCγ2*, *PKD2*, and *PI4KIIIβ* ON-TARGETplus SMARTpool
286 siRNAs were purchased from Horizon Discovery (Waterbeach, UK). A list of the siRNAs used in
287 this study is provided in Supplementary Table 2. Electroporation was performed using the NEON
288 Transfection System (Thermo Fisher Scientific) according to the manufacturer's instructions.

289 **Immunofluorescence confocal microscopy**

290 GIST-T1 cells were cultured on poly L-lysine-coated coverslips and fixed with 4%
291 paraformaldehyde (PFA) for 20 min at room temperature. The fixed cells were permeabilised and
292 blocked for 30 min in Dulbecco's phosphate-buffered saline (D-PBS(-)) supplemented with 0.1%
293 saponin and 3% bovine serum albumin (BSA), and then incubated with primary and secondary
294 antibodies for 1 h each. After washing with D-PBS(-), cells were mounted using Fluoromount
295 (Diagnostic BioSystems, Pleasanton, CA, USA). Confocal images were obtained using a
296 FLUOVIEW FV3000 (Olympus, Tokyo, Japan) or TCS SP8 (Leica, Wetzlar, Germany) laser
297 scanning microscope. Composite figures were prepared using FV31S-SW (Olympus), Leica
298 Application Suite X Software (Leica), Photoshop, and Illustrator (Adobe, San Jose, CA, USA).

299 **Immunostaining for PI4P visualisation**

300 GIST-T1 cells were treated with 50 mM NH_4Cl in D-PBS(-) before fixation with 2% PFA.
301 Permeabilisation and staining were performed as previously described. To stain for PI4P, anti-

302 PI4P mouse IgM (Echelon Biosciences, Salt Lake City, UT, USA) and goat Alexa Fluor 488-
303 conjugated anti-mouse IgM (Thermo Fisher Scientific) were used as primary and secondary
304 antibodies, respectively. After washing with D-PBS(-), stained cells were fixed with 2% PFA for
305 15 min, treated with 50 mM NH_4Cl in D-PBS(-), and washed with double distilled water.

306 **Western blotting**

307 Lysates prepared in sodium dodecyl sulphate-polyacrylamide gel electrophoresis (SDS-PAGE)
308 sample buffer were subjected to SDS-PAGE and electrotransferred onto polyvinylidene fluoride
309 membranes. Briefly, 5% skim milk in Tris-buffered saline containing Tween 20 (TBST) was used
310 to dilute the antibodies. For immunoblotting with anti-pKIT Y703, anti-pPLD2 Y169 or Y511,
311 the antibodies were diluted with 3% BSA in TBST. Immunodetection was performed using the
312 Immobilon Western Chemiluminescent HRP Substrate (Sigma-Aldrich). Sequential re-probing of
313 the membranes was performed after complete removal of antibodies with Restore PLUS Western
314 Blot Stripping Buffer (Thermo Fisher Scientific) and/or inactivation of peroxidase by 0.1%
315 sodium azide. The results were analysed using a ChemiDoc XRC+ with Image Lab software (Bio-
316 Rad, Hercules, CA, USA).

317 **Immunoprecipitation**

318 Lysates from imatinib-treated GIST-T1 cells were prepared in NP-40 lysis buffer supplemented
319 with 50 mM HEPES (pH 7.4), 10% glycerol, 1% NP-40, 4 mM EDTA, 100 mM NaF, 1 mM
320 Na_3VO_4, protease inhibitor cocktail, 2 mM β-glycerophosphate, 2 mM sodium pyrophosphate,
321 and 1 mM phenylmethylsulfonyl fluoride. Immunoprecipitation was performed at 4°C for 5 h

322 using Dynabeads Protein G beads pre-coated with anti-KIT, anti-GGA1, or anti-PLD2 antibodies.
323 Immunoprecipitates were dissolved in SDS-PAGE sample buffer and immunoblotted.

324 **PLD2-MYC transfection**

325 A gene encoding carboxy-terminal MYC-tagged PLD2 (PLD2-MYC), inserted into the pRP
326 vector for expression in mammalian cells, was purchased from VectorBuilder (Yokohama, Japan;
327 vector ID, VB230228-1368ssm). Transient transfection of PLD2-MYC was performed using
328 PEIMAX (Polysciences, Warrington, PA, USA) or JetOPTIMUS (Polyplus-Transfection, Illkirch,
329 France). PLD2-MYC expression was detected by immunoblotting and immunofluorescence using
330 an anti-MYC antibody (71D10).

Data availability

All datasets used and/or analysed in the current study are available from the corresponding author upon reasonable request.

Acknowledgments

This work was supported by a grant-in-aid for Scientific Research from the Japan Society for the Promotion of Science, Japan (24K10370 to Y. O. and 22K08883 to T. N.), a research grant from the Research Foundation for Pharmaceutical Sciences, Japan (to Y. O.), the Japan Foundation for Applied Enzymology, Japan (to Y. O.), the Life Science Foundation of Japan (to Y. O.), and the Foundation for the Promotion of Cancer Research, Japan (to Y. O.).

340 **Author contributions**

341 Y. O. conceived, designed, performed, and analysed the data from all experiments and wrote the
342 manuscript. M. N. performed the immunoblotting and edited the manuscript. R. A. conceived and
343 supervised the project and analysed the data. T. T. provided advice regarding the design of the *in*
344 *vitro* experiments. T. N. provided advice on the design of the *in vitro* experiments and edited the
345 manuscript. All the authors have read and approved the final version of the manuscript.

Funding

The Japan Society for the Promotion of Science (24K10370 to Y. O. and 22K08883 to T. N.). Research Foundation for Pharmaceutical Sciences (to Y. O.). Japan Foundation for Applied Enzymology (Y. O.). Life Science Foundation of Japan (to Y. O.). Foundation for the Promotion of Cancer Research (to Y. O.).

Competing interests

The authors declare no competing interests.

353 **Abbreviations**

354 AML, acute myelogenous leukemia; AP1, adaptor protein-1 complex; ARF, ADP-ribosylation
355 factor; BSA, bovine serum albumin; CAY, CAY10594; CRT, CRT0066101; DMEM, Dulbecco's
356 modified Eagle's medium; D-PBS(-), Dulbecco's phosphate-buffered saline; siRNA, small
357 interfering RNA; ER, endoplasmic reticulum; ERK, extracellular signal-regulated kinase; FCS,
358 fetal calf serum; FGFR, fibroblast growth factor receptor; FLT3-ITD, FMS-like tyrosine kinase
359 3-intenal tandem duplication; GGA, Golgi-associated, γ-adaptin ear-containing, ARF-binding
360 protein; GIST, gastrointestinal stromal tumor; IP, immunoprecipitation; LAMP1, lysosome-
361 associated membrane protein 1; MCL, mast cell leukemia; mut, mutant; NH_4Cl, ammonium
362 chloride; PA, phosphatidic acid; PC-PLD, phosphatidylcholine-selective phospholipase D;
363 PDGFR, platelet-derived growth factor receptor; Pen/Strep, penicillin and streptomycin; PFA,
364 paraformaldehyde; PI3K, phosphatidylinositol-3 kinase; PI4KIIIβ, phosphatidylinositol-4 kinase
365 IIIβ; PI4P, phosphatidylinositol 4-phosphate; PKD, protein kinase D; pKIT, phospho-KIT; PLCγ,
366 phospholipase Cγ; PM, plasma membrane; RTK, receptor tyrosine kinase; SCF-R, stem cell factor
367 receptor; SDS-PAGE, sodium dodecyl-sulfate polyacrylamide gel electrophoresis; siRNA, small
368 interfering RNA; STAT, signal transducer and activator of transcription; TBST, Tris-buffered
369 saline with Tween 20; TfR, transferrin receptor; TGN, *trans*-Golgi network; TKI, tyrosine kinase
370 inhibitor; TRKA, tropomyosin receptor kinase A.

371 **References**

372 1. Lennartsson, J. & Rönnstrand, L. Stem cell factor receptor/c-Kit: from basic science to
373 clinical implications. *Physiol. Rev.* **92,** 1619–1649. (2012).

374 2. Tsai, M., Valent, P. & Galli, S.J. KIT as a master regulator of the mast cell lineage. *J. Allergy*
375 *Clin. Immunol.* **149,** 1845–1854. (2022).

376 3. Thomsen, L. *et al.* Interstitial cells of Cajal generate a rhythmic pacemaker current. *Nat. Med.*
377 **4,** 848–851. (1998).

378 4. Bibi, S. *et al.* Co-operating STAT5 and AKT signaling pathways in chronic myeloid leukemia
379 and mastocytosis: possible new targets of therapy. *Haematologica* **99,** 417–429. (2014).

380 5. Hirota, S. *et al.* Gain-of-function mutations of c-kit in human gastrointestinal stromal tumors.
381 *Science* **279,** 577–580. (1998).

382 6. Nishida, T. *et al.* Familial gastrointestinal stromal tumours with germline mutation of the
383 KIT gene. *Nat. Genet.* **19,** 323–324. (1998).

384 7. Kitamura, Y., Hirota, S. & Nishida, T. Gastrointestinal stromal tumors (GIST): a model for
385 molecule-based diagnosis and treatment of solid tumors. *Cancer Sci.* **94,** 315–320. (2003).

386 8. Rubin, B.P. & Duensing, A. Mechanisms of resistance to small molecule kinase inhibition in
387 the treatment of solid tumors. *Lab. Invest.* **86,** 981–986. (2006).

388 9. Lasota, J. & Miettinen, M. Clinical significance of oncogenic KIT and PDGFRA mutations
389 in gastrointestinal stromal tumours. *Histopathology* **53,** 245–266. (2008).

390 10. Blay, J.Y., Kang, Y.K., Nishida, T. & von Mehren, M. Gastrointestinal stromal tumours. *Nat.*
391 *Rev. Dis. Primers* **18,** 22. (2021).

392 11. Obata, Y. *et al.* Oncogenic Kit signals on endolysosomes and endoplasmic reticulum are
393 essential for neoplastic mast cell proliferation. *Nat. Commun.* **5,** 5715. (2014).
394 12. Obata, Y. *et al.* Oncogenic signaling by Kit tyrosine kinase occurs selectively on the Golgi
395 apparatus in gastrointestinal stromal tumors. *Oncogene* **36,** 3661–3672. (2017).
396 13. Hara, Y. *et al.* M-COPA suppresses endolysosomal Kit-Akt oncogenic signalling through
397 inhibiting the secretory pathway in neoplastic mast cells. *PLOS ONE* **12,** e0175514. (2017).
398 14. Obata, Y., *et al.* Oncogenic Kit signalling on the Golgi is suppressed by blocking secretory
399 trafficking with M-COPA in gastrointestinal stromal tumours. *Cancer Lett.* **415,** 1–10. (2018).
400 15. Obata, Y. *et al.* N822K- or V560G-mutated KIT activation preferentially occurs in lipid rafts
401 of the Golgi apparatus in leukemia cells. *Cell Commun. Signal.* **17,** 114. (2019).
402 16. Obata, Y. *et al.* Golgi retention and oncogenic KIT signaling via PLCγ2-PKD2-PI4KIIIβ
403 activation in gastrointestinal stromal tumor cells. *Cell Rep.* **42,** 113035. (2023).
404 17. Sonoda, H., Okada, T., Jahangeer, S. & Nakamura, S. Requirement of phospholipase D for
405 ilimaquinone-induced Golgi membrane fragmentation. *J. Biol. Chem.* **282,** 34085–34092.
406 (2007).
407 18. Malhotra, V. & Campelo, F. PKD regulates membrane fission to generate TGN to cell surface
408 transport carriers. *Cold Spring Harb. Perspect. Biol.* **3,** a005280. (2011).
409 19. Roussel, É. & Lippé, R. Cellular Protein Kinase D Modulators Play a Role during Multiple
410 Steps of Herpes Simplex Virus 1 Egress. *J. Virol.* **92,** e01486-18. (2018).
411 20. Chen, Y.G. *et al.* Phospholipase D stimulates release of nascent secretory vesicles from the
412 trans-Golgi network. *J. Cell Biol.* **138,** 495–504. (1997).

413 21. Hashimoto, Y. *et al.* Phosphatidic acid metabolism regulates the intracellular trafficking and
414 retrotranslocation of CFTR. *Biochim. Biophys. Acta.* **1783,** 153–162. (2008).
415 22. Brito de Souza, L., Pinto da Silva, L.L., Jamur, M.C. & Oliver, C. Phospholipase D is
416 involved in the formation of Golgi associated clathrin coated vesicles in human parotid duct
417 cells. *PLOS ONE* **9,** e91868. (2014).
418 23. Freyberg, Z., Bourgoin, S. & Shields, D. Phospholipase D2 is localized to the rims of the
419 Golgi apparatus in mammalian cells. *Mol. Biol. Cell* **13,** 3930–3942. (2012)
420 24. Carmon, O. *et al.* Chromogranin A preferential interaction with Golgi phosphatidic acid
421 induces membrane deformation and contributes to secretory granule biogenesis. *FASEB J.*
422 **34,** 6769–6790. (2020).
423 25. Tanguy, E. *et al.* Phospholipase D1-generated phosphatidic acid modulates secretory granule
424 trafficking from biogenesis to compensatory endocytosis in neuroendocrine cells. *Adv. Biol.*
425 *Regul.* **83,** 100844. (2022).
426 26. Kooijman, E.E., Chupin, V., de Kruijff, B. & Burger, K.N. Modulation of membrane
427 curvature by phosphatidic acid and lysophosphatidic acid. *Traffic* **4,** 162–174. (2003).
428 27. Zhukovsky, M.A., Filograna, A., Luini, A., Corda, D. & Valente, C. Phosphatidic acid in
429 membrane rearrangements. *FEBS Lett.* **593,** 2428–2451. (2019).
430 28. Roth, M.G. Molecular mechanisms of PLD function in membrane traffic. *Traffic* **9,** 1233–
431 1239. (2008).
432 29. Nelson, R.K. & Frohman, M.A. Physiological and pathophysiological roles for
433 phospholipase D. *J. Lipid Res.* **56,** 2229–2237. (2015).

434 30. Taguchi, T. *et al.* Conventional and molecular cytogenetic characterization of a new human
435 cell line, GIST-T1, established from gastrointestinal stromal tumor. *Lab. Invest.* **82,** 663–
436 665. (2002).
437 31. Yao, Y. *et al.* Phospholipase D as a key modulator of cancer progression. *Biol. Rev. Camb.*
438 *Philos. Soc.* **95,** 911–935. (2020).
439 32. Lingelem, A.B.D. *et al.* Diacylglycerol kinase and phospholipase D inhibitors alter the
440 cellular lipidome and endosomal sorting towards the Golgi apparatus. *Cell. Mol. Life Sci.* **78,**
441 985–1009. (2021).
442 33. Bi, K., Roth, M.G. & Ktistakis, N.T. Phosphatidic acid formation by phospholipase D is
443 required for transport from the endoplasmic reticulum to the Golgi complex. *Curr. Biol.* **7,**
444 301–307. (1997).
445 34. Brown, H.A., Thomas, P.G. & Lindsley, C.W. Targeting phospholipase D in cancer, infection
446 and neurodegenerative disorders. *Nat. Rev. Drug Discov.* **16,** 351–367. (2017).
447 35. Taraboulos, A., Raeber, A.J., Borchelt, D.R., Serban, D. & Prusiner, S.B. Synthesis and
448 trafficking of prion proteins in cultured cells. *Mol. Biol. Cell* **3,** 851–863. (1992).
449 36. Mayor, S., Presley, J.F. & Maxfield, F.R. Sorting of membrane components from endosomes
450 and subsequent recycling to the cell surface occurs by a bulk flow process. *J. Cell Biol.* **121,**
451 1257–1269. (1993).
452 37. Gomez-Cambronero, J. Phospholipase D in cell signaling: from a myriad of cell functions to
453 cancer growth and metastasis. *J. Biol. Chem.* **289,** 22557–22566. (2014).

454 38. Yamawaki, K. *et al.* FLT3-ITD transduces autonomous growth signals during its biosynthetic
455 trafficking in acute myelogenous leukemia cells. *Sci. Rep.* **11,** 22678. (2021).
456 39. Choudhary, C. *et al.* Mislocalized activation of oncogenic RTKs switches downstream
457 signaling outcomes. *Mol. Cell* **36,** 326–339. (2009).
458 40. Ip, C.K.M. *et al.* Neomorphic PDGFRA extracellular domain driver mutations are resistant
459 to PDGFRA targeted therapies. *Nat. Commun.* **9,** 4583. (2018).
460 41. Bahlawane, C. *et al.* Constitutive activation of oncogenic PDGFRα-mutant proteins
461 occurring in GIST patients induces receptor mislocalisation and alters PDGFRα signalling
462 characteristics. *Cell Commun. Signal.* **13,** 21. (2015).
463 42. Ronchetti, D. *et al.* Deregulated FGFR3 mutants in multiple myeloma cell lines with t(4;14):
464 comparative analysis of Y373C, K650E and the novel G384D mutations. *Oncogene* **20,**
465 3553–3562. (2001).
466 43. Farina, A.R. *et al.* Retrograde TrkAIII transport from ERGIC to ER: a re-localisation
467 mechanism for oncogenic activity. *Oncotarget* **6,** 35636–35651. (2015).
468 44. Schmidt-Arras, D. & Böhmer, F.D. Mislocalisation of Activated Receptor Tyrosine Kinases
469 - Challenges for Cancer Therapy. *Trends Mol. Med.* **26,** 833–847. (2020).
470 45. Frazier, N.M., Brand, T., Gordan, J.D., Grandis, J. & Jura, N. Overexpression-mediated
471 activation of MET in the Golgi promotes HER3/ERBB3 phosphorylation. *Oncogene* **38,**
472 1936–1950. (2018).
473 46. Matsuda, D. *et al.* Involvement of Golgi-associated Lyn tyrosine kinase in the translocation
474 of annexin II to the endoplasmic reticulum under oxidative stress. *Exp. Cell Res.* **312,** 1205–

475 1217. (2006).

476 47. Pulvirenti, T. *et al.* A traffic-activated Golgi-based signalling circuit coordinates the secretory
477 pathway. *Nat. Cell Biol.* **10,** 912–922. (2008).

478 48. Sato, I. *et al.* Differential trafficking of Src, Lyn, Yes and Fyn is specified by the state of
479 palmitoylation in the SH4 domain. *J. Cell Sci.* **122,** 965–975. (2009).

480 49. Thomas, J.D. *et al.* Rab1A is an mTORC1 activator and a colorectal oncogene. *Cancer Cell*
481 **26,** 754–769. (2014).

482 50. Chiu, V.K. *et al.* Ras signalling on the endoplasmic reticulum and the Golgi. *Nat. Cell Biol.*
483 **4,** 343–350. (2001).

484 51. Rocks, O., *et al.* An acylation cycle regulates localization and activity of palmitoylated Ras
485 isoforms. *Science* **307,** 1746–1752. (2005).

486 52. Voss, M. *et al*. Phospholipase D stimulation by receptor tyrosine kinases mediated by protein
487 kinase C and a Ras/Ral signaling cascade. *J. Biol. Chem.* **274,** 34691–34698. (1999).

488 53. Schubbert, S., Shannon, K. & Bollag, G. Hyperactive Ras in developmental disorders and
489 cancer. *Nat. Rev. Cancer* **7,** 295–308. (2007).

490 54. Shen, Y., Xu, L. & Foster, D.A. Role for phospholipase D in receptor-mediated endocytosis.
491 *Mol. Cell. Biol.* **21,** 595–602. (2001).

492 55. Mor, A. *et al.* The lymphocyte function-associated antigen-1 receptor costimulates plasma
493 membrane Ras via phospholipase D2. *Nat. Cell Biol.* **9,** 713–719. (2007).

494 56. Bullen, H.E. & Soldati-Favre, D. A central role for phosphatidic acid as a lipid mediator of
495 regulated exocytosis in apicomplexa. *FEBS Lett.* **590,** 2469–2481. (2016).

496 57. Koike, T., Mizutani, T., Hirai, K., Morita, Y. & Nozawa, Y. SCF/c-kit receptor-mediated
497 arachidonic acid liberation in rat mast cells. Involvement of PLD activation associated
498 tyrosine phosphorylation. *Biochem. Biophys. Res. Commun.* **197,** 1570–1577. (1993).
499 58. Koike, T., Hirai, K., Morita, Y. & Nozawa, Y. Stem cell factor-induced signal transduction in
500 rat mast cells. Activation of phospholipase D but not phosphoinositide-specific
501 phospholipase C in c-kit receptor stimulation. *J. Immunol.* **151,** 359–366. (1993).
502 59. Ktistakis, N.T., Brown, H.A., Waters, M.G., Sternweis, P.C. & Roth, M.G. Evidence that
503 phospholipase D mediates ADP ribosylation factor-dependent formation of Golgi coated
504 vesicles. *J. Cell Biol.* **134,** 295–306. (1996).
505 60. Sztul, E. *et al.* ARF GTPases and their GEFs and GAPs: concepts and challenges. *Mol. Biol.*
506 *Cell* **30,** 1249–1271. (2019).
507 61. Natsume M. *et al.* Brefeldin A and M-COPA block the export of RTKs from the endoplasmic
508 reticulum via simultaneous inactivation of ARF1, ARF4, and ARF5. *J. Biol. Chem.* **300,**
509 107327. (2024).
510 62. Takahashi, T. *et al.* Genomic and transcriptomic analysis of imatinib resistance in
511 gastrointestinal stromal tumors. *Genes Chromosomes Cancer* **56,** 303–313. (2017).
512 63. Foster, D.A., Salloum, D., Menon, D. & Frias, M.A. Phospholipase D and the maintenance
513 of phosphatidic acid levels for regulation of mammalian target of rapamycin (mTOR). *J. Biol.*
514 *Chem.* **289,** 22583–22588. (2014).
515 64. Bauer, S., Duensing, A., Demetri, G.D. & Fletcher, J.A. KIT oncogenic signaling
516 mechanisms in imatinib-resistant gastrointestinal stromal tumor: PI3-kinase/AKT is a crucial

517 survival pathway. *Oncogene* **26,** 7560–7568. (2007).

518 65. Furitsu, T. *et al.* Identification of mutations in the coding sequence of the proto-oncogene c-
519 kit in a human mast cell leukemia cell line causing ligand-independent activation of c-kit
520 product. *J. Clin. Invest.* **92,** 1736–1744. (1993).

521 **Figure Legends**

522 **Figure 1. KIT^{mut} is trapped in the Golgi/TGN area in a manner dependent on PLD activity**
523 **in GIST cells.**

524 (**a**) GIST-T1 cells were treated with 20 μM CAY10594 (CAY, a PLD inhibitor) for 4 h, then
525 immunostained for KIT (green) and golgin97 (Golgi marker, red). Insets show magnified images
526 of the Golgi/TGN area. Scale bars, 20 μm. Note that KIT disappeared from the Golgi/TGN area
527 in the presence of CAY10594. (**b**) GIST-T1 cells were treated with CAY10594 for the indicated
528 periods and then immunoblotted. pKIT^{Y703}, phospho-KIT Y703; pPKD2^{S876}, phospho-PKD2
529 S876. Note that the release of KIT^{mut} from the Golgi/TGN area by CAY10594 treatment
530 inactivated AKT and STAT5 without decreasing pPKD2^{S876}. (**c**) GIST-T1 cells were treated with
531 1% 1-butanol (inhibits PLD activity) for 8 h and then immunoblotted. (**d**) Imatinib-resistant cell
532 lines, GIST-R9 cells (left) and GIST430 cells (right), were treated with CAY10594 for 8 h and
533 then immunoblotted.

534 **Figure 2. CAY10594-induced reduction of KIT is due to lysosomal degradation.**

535 (**a**) GIST-T1 cells were treated with 20 μM CAY10594 (CAY, a PLD inhibitor) and/or 20 mM
536 NH_4Cl (inhibits lysosomal proteases) for (**a**) 16 h or (**b**) 4 h. (**a**) Lysates were immunoblotted for
537 KIT, phospho-KIT Y703 (pKIT^{Y703}), transferrin receptor (TfR, a recycling endosome protein),
538 and β-actin. (**b**) Cells were immunostained with KIT (green) and LAMP1 (lysosome-associated
539 membrane protein 1, red). Scale bars, 20 μm. Note that KIT was found in lysosomes in GIST cells
540 treated with CAY10594 plus NH_4Cl.

541 **Figure 3. PLD2 is a downstream molecule of KIT^{mut} in GIST-T1 cells.**

542 (**a**) GIST-T1 cells were transfected with *PLD1*-targeted siRNA or *PLD2*-targeted siRNA and
543 cultured for 30 h. Lysates were immunoblotted with the indicated antibodies. pKIT^{Y703}, phospho-
544 KIT Y703; pPKD2^{S876}, phospho-PKD2 S876. ND, not detected. Note that PLD2 knockdown
545 phenocopied CAY10594 treatment in GIST-T1 cells. (**b**, **c**) GIST-T1 cells were treated with
546 imatinib (IMA, a KIT tyrosine kinase inhibitor) for 8 h. (**b**) Lysates were immunoblotted.
547 pPLD2^{Y169}, phospho-PLD2 Y169; pPLD2^{Y511}, phospho-PLD2 Y511. (**c**) KIT (left) or PLD2
548 (right) in cells treated with 200 nM imatinib was immunoprecipitated. The immunoprecipitates
549 were immunoblotted. IP, immunoprecipitation. (**d**, **e**) Kasumi-1 (AML, *KIT*^{N822K}), HMC-1.2
550 (MCL, *KIT*^{D816V}), or MOLM-14 cells (AML, *FLT3*^{ITD}) were transfected with PLD1-targeted
551 siRNA or PLD2-targeted siRNA and cultured for 48 h. Lysates were immunoblotted with the
552 indicated antibodies. ND, not detected.

553 **Figure 4. In GIST-T1 cells, PKD2, but not PI4KIIIβ, is an upstream molecule of PLD2.**

554 (**a**) GIST-T1 cells were transfected with the indicated siRNAs and cultured for 30 h. Lysates were
555 immunoblotted with the indicated antibodies. pPLD2^{Y511}, phospho-PLD2 Y511. (**b**) GIST-T1
556 cells were treated with 200 nM imatinib (IMA, a KIT tyrosine kinase inhibitor), 10 μM
557 CRT0066101 (CRT, a PKD inhibitor), 20 μM PIK-93 (a PI4KIIIβ inhibitor), or 20 μM CAY10594
558 (CAY, a PLD inhibitor) for 4 h. Cells were immunostained with anti-PI4P (green) and golgin97
559 (TGN marker, magenta). Arrowheads indicate the Golgi/TGN area. Scale bars, 20 μm. Note that
560 PI4P in the Golgi/TGN area was decreased by treatment of imatinib, CRT0066101, and PIK-93,
561 whereas it was retained in the presence of CAY10594. (**c**) GIST-T1 cells were treated with 20 μM

562 PIK-93, 10 μM CRT0066101, or CAY10594 for 8 h. GGA1 was immunoprecipitated with anti-
563 GGA1 antibody. The immunoprecipitates were immunoblotted for GGA1 and γ-adaptin. IP,
564 immunoprecipitation. (**d**) PKD2 separately activates PLD and PI4KIIIβ in GIST cells. Both
565 enzymatic products, PI4P and phosphatidic acid (PA), directly or indirectly play a role in the
566 association of GGA1 with AP1, which is important for Golgi/TGN retention of KIT^{mut}. If these
567 pathways are blocked, KIT^{mut} is released from the Golgi/TGN region, resulting in degradation in
568 lysosomes.

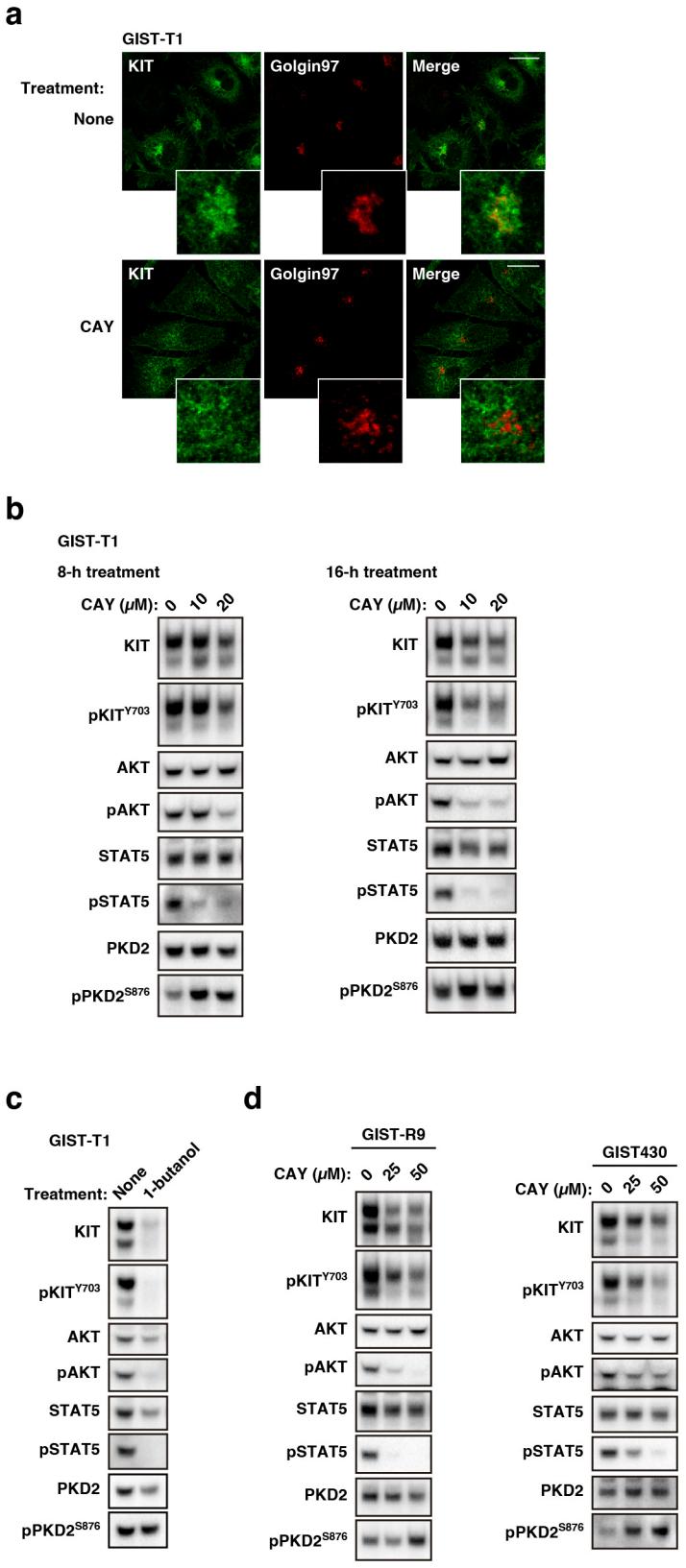
a
GIST-T1
Treatment:
None
CAY
KIT
Golgin97
Merge
b
GIST-T1
8-h treatment
16-h treatment
CAY (μM): 0 10 20
KIT
pKIT Y703
AKT
pAKT
STAT5
pSTAT5
PKD2
pPKD2 S876
c
GIST-T1
Treatment: None 1-butanol
d
GIST-R9
GIST430
CAY (μM): 0 25 50

Figure-1

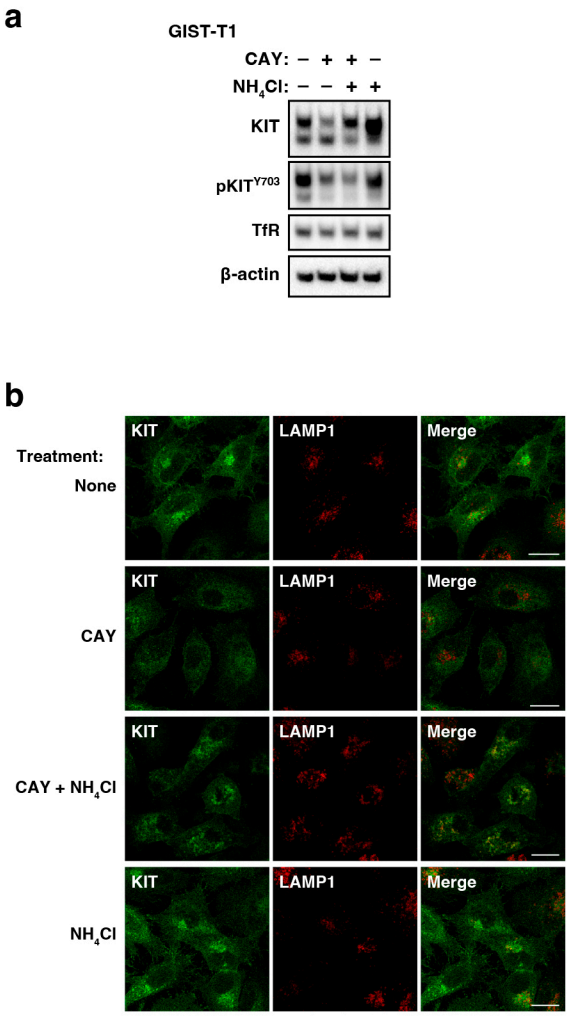
a
GIST-T1
CAY: − + + −
NH4Cl: − − + +
KIT
pKITY703
TfR
β-actin
b
Treatment:
None
CAY
CAY + NH4Cl
NH4Cl
KIT
LAMP1
Merge

Figure-2

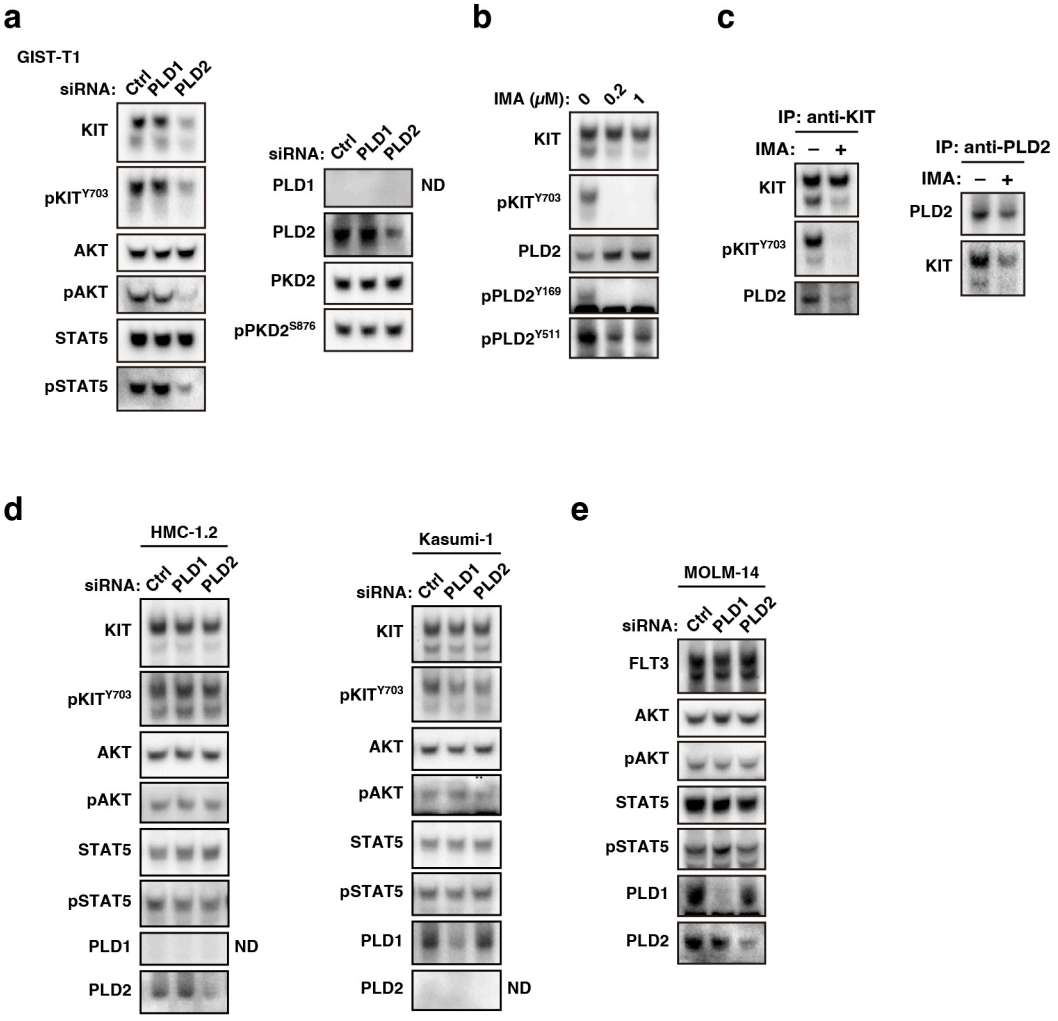
a
GIST-T1
siRNA: Ctrl PLD1 PLD2
KIT
pKIT^{Y703}
AKT
pAKT
STAT5
pSTAT5
siRNA: Ctrl PLD1 PLD2
PLD1
ND
PLD2
PKD2
pPKD2^{S876}
b
IMA (μM): 0 0.2 1
KIT
pKIT^{Y703}
PLD2
pPLD2^{Y169}
pPLD2^{Y511}
c
IP: anti-KIT
IMA: – +
KIT
pKIT^{Y703}
PLD2
IP: anti-PLD2
IMA: – +
PLD2
KIT
d
HMC-1.2
siRNA: Ctrl PLD1 PLD2
KIT
pKIT^{Y703}
AKT
pAKT
STAT5
pSTAT5
PLD1
ND
PLD2
Kasumi-1
siRNA: Ctrl PLD1 PLD2
KIT
pKIT^{Y703}
AKT
pAKT
STAT5
pSTAT5
PLD1
PLD2
ND
e
MOLM-14
siRNA: Ctrl PLD1 PLD2
FLT3
AKT
pAKT
STAT5
pSTAT5
PLD1
PLD2

Figure-3

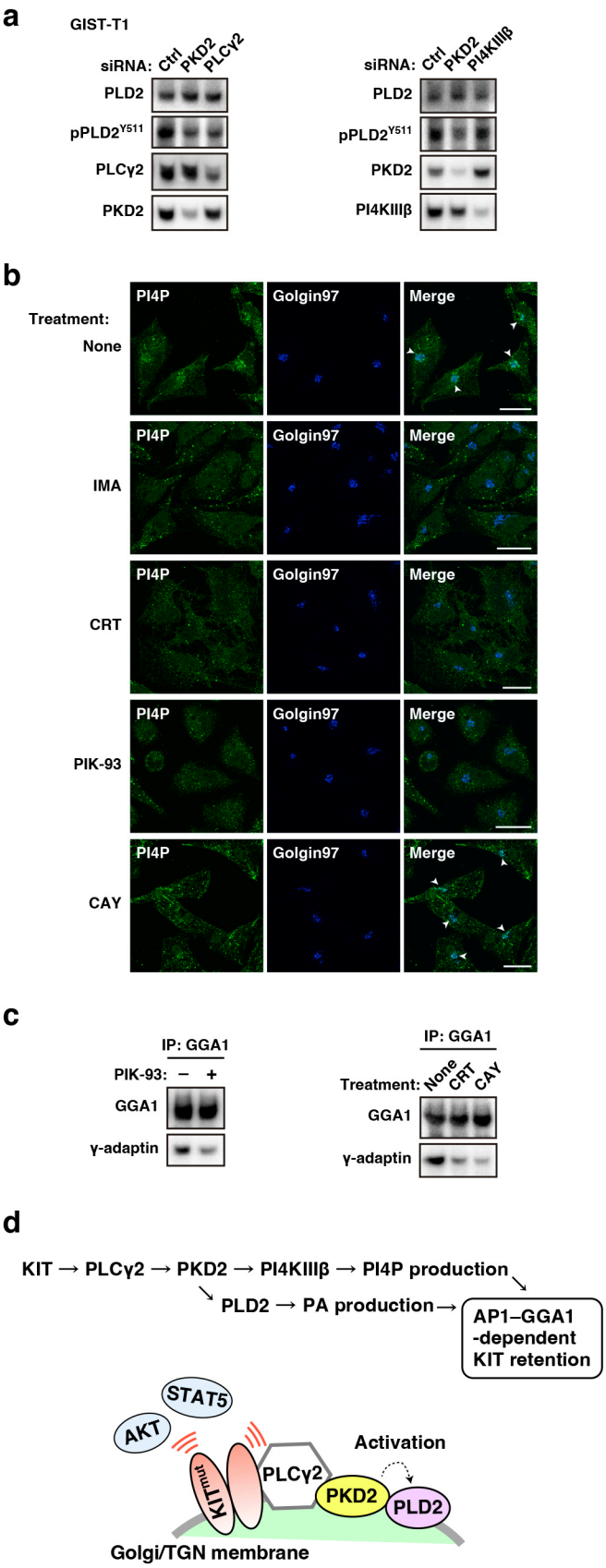
a
GIST-T1
siRNA: Ctrl PKD2 PLCγ2
PLD2
pPLD2Y511
PLCγ2
PKD2
siRNA: Ctrl PKD2 PI4KIIIβ
PLD2
pPLD2Y511
PKD2
PI4KIIIβ
b
Treatment:
None
IMA
CRT
PIK-93
CAY
PI4P
Golgin97
Merge
c
IP: GGA1
PIK-93: − +
GGA1
γ-adaptin
IP: GGA1
Treatment: None CRT CAY
GGA1
γ-adaptin
d
KIT → PLCγ2 → PKD2 → PI4KIIIβ → PI4P production
PLD2 → PA production →
AP1–GGA1 -dependent KIT retention
STAT5
AKT
KITmut
PLCγ2
PKD2
PLD2
Activation
Golgi/TGN membrane

Figure-4